

Comparison between Fenton oxidation process and electrochemical oxidation for PAH removal from an amphoteric surfactant solution

Lan-Huong Tran · Patrick Drogui ·
Guy Mercier · Jean-François Blais

Received: 10 October 2009 / Accepted: 27 March 2010 / Published online: 16 April 2010
© Springer Science+Business Media B.V. 2010

Abstract The decomposition of polycyclic aromatic hydrocarbons in a creosote oily solution and in synthetic solutions containing naphthalene and pyrene was investigated in the presence of an amphoteric surfactant using electrooxidation by comparison to Fenton oxidation process. Electrolysis was carried out using a parallelepipedic electrolytic 1.5-L cell containing five anodes (expanded titanium covered with ruthenium) and five cathodes (stainless steel) alternated in the electrode pack, whereas Fenton oxidation process was carried out in 500 mL Erlenmeyer glass-flasks in which H_2O_2 and Fe^{2+} were added. Using electrochemical oxidation, the sum concentration of 16 polycyclic aromatic hydrocarbons investigated could be optimally diminished by up to 80–82% by applying a current density of 9.23 mA cm^{-2} and a pH of 4.0 or 7.0 for 90-min reaction period. By comparison, the best yield (46%) of Fenton oxidation process for polycyclic aromatic hydrocarbons degradation was recorded by using $\text{H}_2\text{O}_2/\text{Fe}^{2+}$ molar ratio of 11.0 and a pH of 4.0.

Keywords Polycyclic aromatic hydrocarbon · Electrochemical degradation · Fenton oxidation · Hydroxyl radical · Ruthenium oxide electrode · Surfactant

Abbreviations

ACA	Acenaphthene
ACN	Acenaphthylene
ANT	Anthracene
AOP	Advanced oxidation process
AOPs	Advanced oxidation processes
BAA	Benzo(a)anthracene
BAP	Benzo(a)pyrene
BJK	Benzo(b,j,k)fluoranthene
BPR	Benzo(ghi)perylene
CAS	Cocoamidopropyl hydroxysultaine
CHR	Chrysene
CMC	Critical micelle concentration
COD	Chemical oxygen demand
COS	Creosote oily solution
DAN	Dibenzo(a,h)anthracene
DOC	Dissolved organic carbon
FLE	Fluoranthene
FLU	Fluorene
GC	Gas chromatograph
INP	Indeno(1,2,3-c,d)pyrene
MEN	2-Methyl naphthalene
MS	Mass spectrometer
MSR	Molar solubilization ratio
NAP	Naphthalene
NIST	National Institute of Standards and Technology
PAH	Polycyclic aromatic hydrocarbons
PHE	Phenanthrene
PVA	Polyvinyl alcohol
PYR	Pyrene
SIFIS	Selected ion and full ion scanning
Ti/BDD	Titanium covered with boron doped diamond
Ti/RuO ₂	Titanium covered with ruthenium oxide
TOC	Total organic carbon

L.-H. Tran · P. Drogui · G. Mercier · J.-F. Blais (✉)
Institut national de la recherche scientifique (Centre Eau,
Terre et Environnement), Université du Québec, 490 rue de la
Couronne, Québec, QC G1K 9A9, Canada
e-mail: blaisjf@ete.inrs.ca

L.-H. Tran
e-mail: lan.huong.tran@ete.inrs.ca

P. Drogui
e-mail: patrick.drogui@ete.inrs.ca

G. Mercier
e-mail: guy_mercier@ete.inrs.ca

1 Introduction

NAP, PYR and other PAHs are ubiquitous pollutants that are very persistent in the environment due to their resistance to biological degradation, namely for PAH that consist of two or more rings [1, 2]. PAHs are generated whenever organic material (e.g., petroleum, coal, tobacco, wood) are combusted, burned, or cooked. Creosote is one of the important sources of PAH release in the environment. Creosote is a distillate of coal tar [3] and it is an excellent fungicide and insecticide [4]. It is commonly used as wood preservative. Creosote-treated woods are widely used as railway sleepers, telephone and power pole and as exterior wood for use in garden [5–8]. Ikarashi et al. [8] reported that creosote contaminated sites have been identified in Canada, United States, Greenland, Denmark, Sweden and the United Kingdom.

The removal of PAH from water is a difficult task due to their low solubility (Table 1), and refractory character but it can be achieved through some treatment methods, such as chemical advanced oxidation processes (AOPs) [2, 9–11], electrochemical oxidation [12, 13] or biological oxidation using microorganisms [14, 15]. AOPs are often used for PAH degradation [9, 11]. The aim of AOPs (including, O_3/H_2O_2 , UV/O_3 , UV/H_2O_2 , H_2O_2/Fe^{2+}) is to produce hydroxyl radical (OH^*), a very powerful oxidant capable of oxidising a wide range of organic compounds with one or more double bonds. Among the AOPs, the Fenton oxidation process (H_2O_2/Fe^{2+} system) represents the most common and simple AOP, which is often employed for the treatment of wastewaters from various industries [11, 16, 17]. This process is generally conducted in very acidic medium (pH 2–3) to prevent iron salts precipitation [2, 18]. The hydroxyl radicals formed degrade organic compounds either by hydrogen abstraction or by hydroxyl addition [2]. An optimal oxidation of the organic can be obtained when the system is applied in presence of an excess of hydrogen peroxide. Tang and Huang [19] have reported a H_2O_2/Fe^{2+} molar ratio of 10:1 to allow for the best degradation of organic pollutants.

Electrochemical oxidation treatment can also be used for PAH degradation. This type of technology has been widely applied for the treatment of different effluents (textile effluents [20], landfill leachate [21, 22], olive oil wastewater and domestic sewage sludge [23], tannery effluent [24, 25] using different electrode materials. The interest of using electrochemical oxidation is based on its capability of reacting on the pollutants by using both direct and indirect effect of electrical current [21, 26]. Direct oxidation may be achieved through mineralization with hydroxyl radical (OH^*) produced by dimensionally stable anodes having high oxygen overvoltage, such as SnO_2 , PbO_2 and IrO_2 [27–29]. In fact, OH^* radicals are

exclusively generated on the anode electrodes from the oxidation of water and organic compounds can be completely transformed or degraded by reaction with adsorbed OH^* radicals. Indirect oxidation can be achieved through electrochemical generation of a mediator in solution (such as, $HClO$, $HBrO$, H_2O_2 , $H_2S_2O_8$, and others) to convert toxic organics to a less harmful product by using graphite or noble metal anodes [26, 30, 31].

Researchers from the Institut National de la Recherche Scientifique du Québec, INRS-ETE (Centre for Water, Earth and Environment) have developed a physicochemical process for extraction of PAH from aluminium wastes [32, 33] and contaminated soils [34, 35]. The process consists in treating industrial wastes using an amphoteric surfactant (CAS) in a flotation cell of Denver type containing 9.1% of pulp density of contaminated waste. The extraction stage allowed recovering a foam concentrate (foam suspension) strongly loaded with PAH, which must be treated before discharge. Therefore, research has focused on a complementary treatment using either Fenton oxidation process or electrochemical oxidation in treating PAH-containing synthetic solution. The most effective process could be then used in conjunction with the physicochemical process described above for PAH extraction from wastes.

This study was carried out to compare Fenton oxidation process and electrochemical oxidation to determine the most cost-effective process in treating COS strongly loaded with PAH. COS has been used in this study as a model solution containing PAH. Subsequently, NAP and PYR synthetic solutions were individually treated to treatment in order to determine the nature of the intermediate products and to elucidate the plausible mechanism of the electrochemical transformation of NAP and PYR.

2 Materials and methods

2.1 Creosote oily solution (COS)

Commercially-available creosote used in this study was provided by Stella-Jones Inc. (Montréal, QC, Canada). It was comprised of 50% (v/v) of creosote and 50% (v/v) of petroleum hydrocarbons. The creosote effluent was prepared in a 100 mL glass-tank containing 30 g of oily-creosote in which 1 g of an amphoteric surfactant (CAS, Chemron, Ohio) was added. Some important characteristics of the CAS surfactant are shown in Table 2. Conditioning was carried out by mixing with a Teflon-covered stirring bar at a speed of 750 rpm for a period of time of 24 h. At the end of the conditioning stage, the suspension was transferred into a 20 L polypropylene tank containing 10 L of distilled water (final concentration = 3.0 g creosote L^{-1}). The resulting suspension constituted the synthetic

Table 1 Physical and chemical properties of PAH identified in the creosote [47]

PAH	Parameters				
	Abbreviation	Molecular structure	Number of aromatic rings	Molecular weight (g mol ⁻¹)	Aqueous solubility (25 °C, mg L ⁻¹)
Naphthalene	NAP	C ₁₀ H ₈	2	128	31.7
2-Methyl naphtalene	MEN	C ₁₁ H ₁₀	2	142	24.6
Acenaphtylene	ACN	C ₁₂ H ₈	3	152	3.93
Acenaphtene	ACA	C ₁₂ H ₁₀	3	154	1.93
Fluorene	FLU	C ₁₃ H ₁₀	3	166	1.83
Phenanthrene	PHE	C ₁₄ H ₁₀	3	178	1.20
Anthracene	ANT	C ₁₄ H ₁₀	3	178	0.076
Fluoranthene	FLE	C ₁₆ H ₁₀	4	202	0.23
Pyrene	PYR	C ₁₆ H ₁₀	4	202	0.077
Benzo(a)anthracene	BAA	C ₁₈ H ₁₂	4	228	0.0094
Chrysene	CHR	C ₁₈ H ₁₂	4	228	0.0018
Benzo(b,j,k)fluoranthene	BJK	C ₂₀ H ₁₂	5	252	0.0015
Benzo(a)pyrene	BAP	C ₂₀ H ₁₂	5	252	0.0016
Dibenzo(a,h)anthracene	DAN	C ₂₂ H ₁₄	5	278	0.0005
Indeno(1,2,3-c,d)pyrene	INP	C ₂₀ H ₁₂	6	276	0.062
Benzo(ghi)perylene	BPR	C ₂₀ H ₁₂	6	276	0.0003

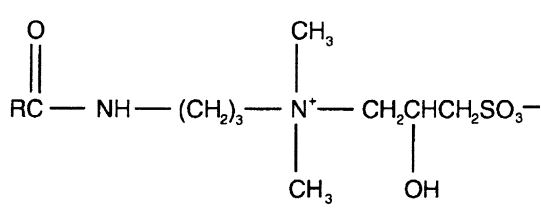
creosote oily solution (COS), which was then settled for at least 24 h in order to separate the insoluble and suspended solids from liquid before electrochemical and chemical oxidation.

2.2 Preparation of individual NAP and PYR solutions

NAP and PYR analytical grade reagents (99% purity) were obtained from Laboratoire Mat (Beauport, QC, Canada).

The first set of experiments consisted to determine the best way of solubilizing NAP and PYR, respectively using the CAS. For that, individual NAP and PYR solutions were prepared in screw-capped Erlenmeyer flasks containing 0.1 g of NAP and PYR, respectively, in which 0.02–8.15 g of CAS surfactant and 300 mL distilled water were added (0.08–27.2 g L⁻¹ of CAS). The mixture was then agitated in a gyratory shaking system (Lab-line, model 3520) at 250 rpm for 24 h at room temperature (around 22 °C). At

Table 2 Characteristics of the CAS surfactant [48, 49]

Cocoamidopropyl hydroxysultaine (CAS)	
Molecular structure	
Formula	CH ₃ (CH ₂) ₁₃ -N(OH)-(CH ₂) ₃ -N ⁺ (CH ₃) ₂ -CH ₂ -CHOH-CH ₂ SO ₃ ⁻
MW ^a (g mol ⁻¹)	452
Density (g mL ⁻¹)	1.11
CMC ^b (mol L ⁻¹)	5 × 10 ⁻⁵
Biodegradability (%)	96%

^a Molecular weight

^b Critical micelle concentration

the end of the conditioning stage, the suspension was filtered Whatman No. 5 membranes (2.5 μm pore diameter, Whatman International Ltd, Maidstone, England) under vacuum in order to separate the insoluble and suspended particles from the suspension. The filtrate was then recovered for analysis of NAP and PYR concentrations.

For electrochemical treatment, individual NAP and PYR synthetic solutions were also prepared using the same procedure by imposing 8.15 g of CAS surfactant in the presence of 0.1 g of NAP and PYR, respectively, and 300 mL distilled was added. After agitation and vacuum filtration of the suspension, the filtrate was then transferred into a tank and diluted to 2.0 L of distilled water (final concentration of CAS = 4.1 g L^{-1}). These synthetic NAP and PYR solutions were agitated for a 30 min before electrochemical treatment. The initial concentrations of NAP and PYR were 106 and 54 mg L^{-1} , respectively.

2.3 Fenton oxidation

Experiments were conducted at room temperature in 500 mL Erlenmeyer glass-flasks, covered with aluminum foil to avoid any photolytic degradation. All the experiments were done in duplicate. For all assays, a working volume of 250 mL of COS was used. COS was mixed by a magnetic agitator using a Teflon-covered stirring bar at 200–300 rpm. Initial pH was adjusted between 2 and 9 using sulphuric acid (H_2SO_4 , 5 mol L^{-1}) or sodium hydroxide (NaOH , 2 mol L^{-1}). Sodium hydroxide and sulphuric acid were analytical grade reagents and supplied by Fisher Scientific. The ferrous iron and hydrogen peroxide solutions, freshly prepared in stock concentrations, were successively added. Ferrous iron was added as $\text{FeSO}_4 \cdot 7\text{H}_2\text{O}$ (Laboratoire Mat, Beauport, QC, Canada). A stock solution (15 $\text{g Fe}^{2+} \text{L}^{-1}$) was prepared with milli-Q water at a pH 2 to avoid ferrous ions precipitation. A fixed concentration of 0.90 $\text{g Fe}^{2+} \text{L}^{-1}$ (1.7 $\text{mol Fe}^{2+} \text{L}^{-1}$) was imposed during the tests, while various concentrations of hydrogen peroxide were tested. Hydrogen peroxide was provided by Fisher Scientific (H_2O_2 , 30% v/v). The stock solution of H_2O_2 was also prepared with prepared milli-Q water at a concentration of 50 $\text{g H}_2\text{O}_2 \text{L}^{-1}$. Hydrogen peroxide concentrations varied from 0.06 to 0.60 g L^{-1} (1.7–17.6 mol L^{-1}), while $\text{H}_2\text{O}_2/\text{Fe}^{2+}$ molar ratios ranged between 1.1 and 11. Time zero was sampled just before the addition of hydrogen peroxide to the COS. The Fenton's reaction was then started upon addition of H_2O_2 . At the end of the treatment (after 60 min of agitation), an aliquot (250 mL) was withdrawn and conditioned before residual PAH analysis.

2.4 Electrochemical oxidation

Electrochemical oxidation of PAH in synthetic solution was carried out in a batch electrolytic cell made of acrylic

material with a dimension of 12 cm (width) \times 12 cm (length) \times 19 cm (depth) (Fig. 1). The electrode sets (anode and cathode) consisted of ten parallel plates of metal with a distance inter-electrode of 1 cm. Five anodes and five cathodes alternated in the electrode pack. The electrodes were placed in stable position and submerged in COS. The anodes were made of expanded titanium (Ti) covered with ruthenium oxide (RuO_2), each one having a solid surface area of 65 cm^2 and a void area of 45 cm^2 . The cathodes were made of stainless steel plates (SS, 316L) of 10 cm width and 11 cm height. The electrodes were placed 2 cm from the bottom of the cell. Mixing in the cell was achieved by a Teflon-covered stirring bar installed between the set of electrodes and the bottom of the cell. For all tests, a working volume of 1.5 L was used. The anodes and cathodes were connected, respectively to the positive and negative outlets of a DC power supply Xantrex XFR 40-70 (Aca Tmetrix, Mississauga, ON, Canada). During the set of electrochemical oxidation experiments an addition of sodium sulphate (0.5 $\text{g Na}_2\text{SO}_4 \text{L}^{-1}$) was necessary to increase the electrical conductivity. The electrochemical cells were operated under galvanostatic conditions, with current densities varying from 4.0 to 13 mA cm^{-2} applied for 90 min. Current was held constant for each run. The influence of pH values ranging from 2.0 to 9.0 was tested. Between two tests, electrolytic cell (including the electrodes) was cleaned with 5% (v/v) nitric acid solution for at least 30 min and then rubbed with a sponge and rinsed with tap water.

2.5 Extraction and purification procedure

After application of Fenton and electrochemical oxidation processes in the synthetic solutions, the residual PAH contents were separated from the aqueous suspensions by extraction and purification on a solid phase using polypropylene-cartridges (Enviro-Clean sorbents, United Chemical Technology Inc.) before analyses. The Enviro-Clean polypropylene-cartridge was successively conditioned by rinsing with 10 mL of dichloromethane (99.9% ACS reagent, EMD chemicals Inc., USA), 10 mL of methanol (99.8% reagent, Fisher Scientific, Canada) and 10 mL of distilled water. Subsequently, 250 mL of samples (treated and untreated synthetic solutions) containing 10 mL of methanol were loaded onto the cartridge where they are entirely filtered drip. PAH retained on the polypropylene-cartridge were then eluted with 10 mL of dichloromethane. After elution, the sample was transferred into a filter containing anhydrous MgSO_4 (EMD chemicals Inc., USA) in order to eliminate all traces of water, followed by evaporation of dichloromethane using a rotary evaporator (Büchi Rotavapor-R, Rico Instrument Co.). The extraction solution was diluted with dichloromethane, and

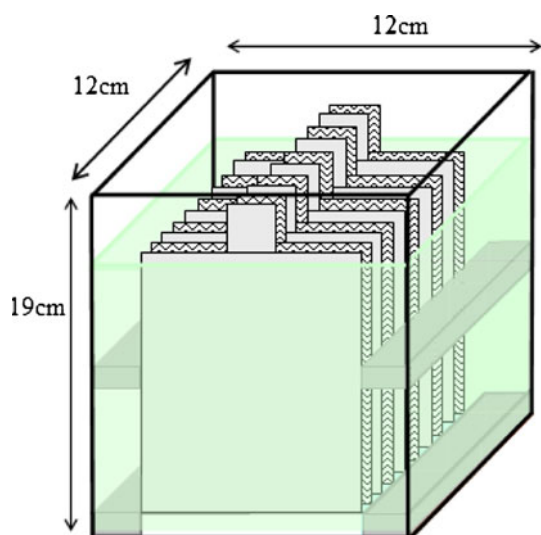


Fig. 1 Electrolytic cell

a series of diluted solution ($1 \times 10 \times 100$) was prepared before analyses.

2.6 Gas chromatographic analysis

PAHs were quantified using a Perkin Elmer 500 gas chromatograph (GC) on a VF-5MS-FS column (0.25 mm diameter, 30 m long and 0.25 μm film thickness) coupled to a Perkin Elmer Clarus 500 series mass spectrometer detector operated with a mass range between m/z 50 and 450. The GC column temperature was programmed as follows: it was first maintained at 80 $^{\circ}\text{C}$ for 2 min, then heated at a rate of 15 $^{\circ}\text{C min}^{-1}$ up to 220 $^{\circ}\text{C}$ and then heated at a rate of 5 $^{\circ}\text{C min}^{-1}$ up to 320 $^{\circ}\text{C}$, after which it was held at this temperature for 5 min. The injection temperature was maintained at 250 $^{\circ}\text{C}$. The carrier gas was helium and column flow was maintained at 2.0 mL/min. A PAH mixture containing 16 PAHs at a concentration of 1 000 mg L^{-1} in dichloromethane-benzene (3:1) (Supelco, Canada) was used as a PAH standard.

2.7 Formation of oxidation by-products

For identification of by-products formed during PAH oxidation, due to the low sensitivity of the detectors used, pre-concentration of the aqueous solution was performed by solid-phase extraction onto polypropylene-cartridges (Enviro-Clean sorbents, United Chemical Technology Inc). Cartridges were conditioned successively with 10 mL aliquots of dichloromethane, methanol and milli-Q water and PAH were eluted with 10 mL dichloromethane. The obtained fractions were analyzed using a Perkin Elmer 500 gas chromatograph (GC) coupled to a mass spectrometer (MS) equipped with a simultaneous Selected ion and full

ion scanning (SIFIS). It is worth noting that by-products were only identified while treating NAP and PYR synthetic solution by means of electrochemical oxidation process. Full scan ion monitoring is by far the most prevalent mode of operation often used for semi-volatile organic compound detection. Indeed, by-products from NAP and PYR oxidation were identified in full scans mode and by using the help of National Institute of Standards and Technology (NIST) library. It covers the necessary mass range and provides classical spectra that can be library searched for positive identification.

2.8 Analytical techniques

The pH was determined using a pH-meter (Fisher Acumet model 915) equipped with a double-junction Cole-Palmer electrode with Ag/AgCl reference cell. A conductivity meter (Oakton Model 510) was used to determine the ionic conductivity of the effluent. The temperature of treated-effluent was monitored using a thermo-meter (Cole-Parmer model Thermo scientific Ertco). COD was determined by Hach COD method.

2.9 Cost assessment

The economic study included chemical and energy consumption. The energy consumed was estimated at a cost of 0.06 US\$ kWh^{-1} , which corresponded to the cost in the province of Quebec (Canada). The electrolyte (Na_2SO_4 industrial grade) provided by Laboratoire Mat (Beauport, QC, Canada) was estimated at a cost of 0.30 US\$ kg^{-1} . Unitary costs of 1,600 US\$ t^{-1} H_2O_2 and 100 US\$ t^{-1} $\text{FeSO}_4 \cdot 7\text{H}_2\text{O}$ were also considered for Fenton reagents. The total cost was evaluated in terms of U.S. dollars spent per cubic meter of treated solution (US\$ m^{-3}).

3 Results and discussion

3.1 PAH oxidation in COS using Fenton oxidation

Experiments were first conducted using Fenton oxidation in COS. Results obtained for different experiments are shown in Table 3 and compared to the initial solution (i.e., no reagent addition). 16 PAH were investigated in the creosote solution and were comprised of different number of aromatic rings (2-, 3-, 4-, 5- and 6-ring PAH). The lowest residual concentration of PAH in solution was obtained while imposing a $\text{H}_2\text{O}_2/\text{Fe}^{2+}$ ratio of 11.0 with a percentage of PAH degradation of 44.7%. The residual total PAH concentrations decreased while increasing $\text{H}_2\text{O}_2/\text{Fe}^{2+}$ ratio. It can also be seen that 3-ring PAH (ACN, ACA, FLU, PHE and ANT) were present in the highest residual

concentration with the percentage of degradation ranging from 7.4 to 42%. By comparison, the yields of degradation of the 4-ring PAH (FLE, PYR, BAA and CHR) ranged between 6.0 and 40%, whereas 5.3 to 44% were recorded with 2-ring PAH (NAP and MEN). The yields of degradation of the 5-ring PAH (BJK, BAP and DAN) ranged between 4.7 and 58%. The lowest yields of PAH degradation from creosote were recorded for 6-ring PAH (INP and BPR) with the percentage ranging from 1.2 to 30%. Using a $\text{H}_2\text{O}_2/\text{Fe}^{2+}$ ratio of 11.0, the rates of PAH degradation (around 40–44%) were quite similar regardless of the number of aromatic rings (2-, 3- and 4-ring PAH) by considering only the compounds present in the highest concentration in creosote solution. The highest yields of PAH degradation recorded at a high $\text{H}_2\text{O}_2/\text{Fe}^{2+}$ ratio of 11 were quite similar to those obtained by Flotron et al. [2] while studying Fenton's reagent process for removal of sorbed PAH from soil, sludge and sediment samples. They studied the oxidation system in the presence of hydrogen peroxide (i.e., $\text{H}_2\text{O}_2/\text{Fe}^{2+} = 10$), and 60% of benzo[a]pyrene was degraded; $\text{H}_2\text{O}_2/\text{Fe}^{2+} = 10$ values being the theoretically optimal ratio according to Tang and Huang (1996). The treatment cost was estimated to $1.28 \text{ \$ m}^{-3}$ (including only the chemical costs, H_2O_2 and FeSO_4) with this chemical ratio.

To investigate the effect of initial pH on the removal efficiency, initial pH of the COS was adjusted between 2 and 9 using H_2SO_4 and NaOH . In addition, a control assay was carried out without pH adjustment (original pH was around 5.8). During these assays, the $\text{H}_2\text{O}_2/\text{Fe}^{2+}$ ratio was maintained at 11.0 and a retention time of 60 min. The results are shown in Table 4. It was found that COS having an initial pH close to pH 4.0 was more favorable for PAH reduction (PAH removal of 49% were recorded), compared to 42% recorded with the original pH or with an initial pH of 9.0. This is consistent with the results of Goel et al. [11] while oxidizing NAP using Fenton's oxidation process. The best results (NAP removal of 99%) were obtained at a pH 4.0 in the presence of $30 \text{ mg Fe}^{2+} \text{ L}^{-1}$ and a concentration of hydroxide peroxide varying between 10 and 12 mg L^{-1} . The efficiency of the process depended strongly on the composition of effluent and the concentration of pollutants. In the case of Goel et al. [11], author used a synthetic NAP solution (only two aromatic rings) with an initial concentration of $9.8 \pm 1.5 \text{ mg NAP L}^{-1}$. By comparison, COS submitted to chemical oxidation contained different types of aromatic rings (two to six aromatic rings) and the initial concentration of total PAH varied from 340 to 360 mg L^{-1} (35–37 times higher than that tested by Goel et al. [11]). This is one of the reasons for which the rates of PAH removal were lower than that receded by Goel et al. [11].

3.2 PAH oxidation in COS using electrochemical oxidation

We compared Fenton oxidation process to electrochemical treatment using Ti/RuO_2 anodes. Residual PAH concentration and PAH removal were examined as a function of current density. The residual PAH concentrations ($80\text{--}111 \text{ mg L}^{-1}$) recorded at the end of the treatment were lower than those measured using Fenton's oxidation process ($209\text{--}340 \text{ mg L}^{-1}$). The yields of PAH degradation increased with current density until 9.23 mA cm^{-2} and then remained quite stable at 12.3 mA cm^{-2} . Using a current density of 9.23 mA cm^{-2} , the rates of PAH degradation (around 81–84%) were quite similar regardless of the number of aromatic rings (2-, 3-, 4-, 5- and 6-ring PAH). The rates of electrochemical degradation of PAH in COS were approximately two times higher than that recorded while applying Fenton's chemical oxidation process using a $\text{H}_2\text{O}_2/\text{Fe}^{2+}$ ratio of 11. This can be explained by two main factors. Firstly, the anodic oxidation of pollutant occurs heterogeneously. Most of PAH compound are hydrophobic compounds so that they can be easily adsorbed on the anode electrode surface and then be effectively oxidized there. Secondly, in our experimental conditions, electrochemical treatment using Ti/RuO_2 anode and operated at a current density of 9.23 mA cm^{-2} was probably more effective in producing hydroxyl radical than Fenton's oxidation process operated at $\text{H}_2\text{O}_2/\text{Fe}^{2+}$ ratio of 11.0. Likewise, electrochemical system provides a constant supply of hydroxyl radicals versus Fenton's process in which H_2O_2 is added only once. However, the treatment cost of electrochemical treatment ($5.11 \text{ US\$ m}^{-3}$) operated at the optimal current density of 9.23 mA cm^{-2} was four times higher than that ($1.28 \text{ US\$ m}^{-3}$) recorded while applying Fenton's oxidation process using $\text{H}_2\text{O}_2/\text{Fe}^{2+}$ molar ratio of 11.0. The removal efficiency at four different initial pH values (2.0, 4.0, 7.0, and 9.0) was also investigated. During these assays, the current density was maintained at 9.23 mA cm^{-2} and a retention time of 90 min was imposed. The results are shown in Table 4. It was found that COS having an initial pH close to the neutral value (pH 7.0) was more favorable for PAH reduction (PAH removal of 81 and 84% were recorded, respectively). This is consistent with the results of Yavuz and Kaporal [36] while oxidizing phenol using ruthenium mixed metal oxide electrode. They reported that electrooxidation around pH 7.0 was more effective in removing phenol, compared to pH 3.0 and pH 11.0. However, one study showed that the pH effect is not significant while oxidizing orange II dye on Ti/BDD anode at a current density imposed of 200 mA m^{-2} [37].

Table 3 Comparison between Fenton oxidation and electrochemical oxidation during the treatment of creosote oily solution

PAH	Fenton oxidation					Electrochemical oxidation					
	Initial	H ₂ O ₂ /Fe ²⁺ molar ratios				Initial	Current densities (mA cm ⁻²)				
		1.1	2.2	4.4	6.6		11.0	4.62	6.15	9.23	12.30
2-ring PAH											
NAP (mg L ⁻¹)	27.5	26.4	25.8	17.4	16.4	14.2	70.1	21.7	21.7	13.6	11.5
MEN (mg L ⁻¹)	30.2	28.2	27.8	25.2	27.8	17.8	53.7	13.0	11.6	8.83	7.30
Sum (mg L ⁻¹)	57.7	54.6	53.6	42.6	44.2	32.0	124	34.7	33.3	22.4	18.8
3-ring PAH											
ACN (mg L ⁻¹)	2.26	2.12	2.08	1.20	1.08	1.02	3.02	1.52	1.08	0.68	0.66
ACA (mg L ⁻¹)	32.4	32.4	32.0	28.6	24.2	16.0	57.1	12.2	11.1	9.40	9.59
FLU (mg L ⁻¹)	39.6	33.3	32.2	24.2	22.6	19.4	38.8	9.87	10.1	9.51	9.12
PHE (mg L ⁻¹)	67.7	57.3	56.8	44.3	43.3	39.6	84.4	22.4	21.9	17.7	18.2
ANT (mg L ⁻¹)	92.1	91.6	88.4	90.8	91.4	59.0	15.3	4.09	4.21	2.95	3.63
Sum (mg L ⁻¹)	234	217	211	189	183	135	199	50.1	48.4	40.2	41.2
4-ring PAH											
FLE (mg L ⁻¹)	36.8	34.0	32.4	31.8	35.2	24.8	40.5	10.7	10.6	8.42	8.99
PYR (mg L ⁻¹)	16.9	16.1	16.2	12.0	13.0	8.40	31.5	8.55	8.07	5.91	5.53
BAA (mg L ⁻¹)	3.91	3.80	3.46	2.48	2.49	2.32	6.02	2.29	2.28	1.26	1.76
CHR (mg L ⁻¹)	5.92	5.80	5.67	3.90	3.60	2.40	8.31	2.26	2.48	1.78	1.94
Sum (mg L ⁻¹)	63.5	59.7	57.7	50.2	54.3	37.9	86.3	23.8	23.4	17.4	18.2
5-ring PAH											
BJK (mg L ⁻¹)	2.93	2.80	2.60	1.80	2.00	1.22	5.86	1.43	1.37	1.25	1.24
BAP (mg L ⁻¹)	4.76	4.54	4.28	3.89	3.56	1.95	2.23	0.62	0.55	0.47	0.49
DAN (mg L ⁻¹)	0.11	0.091	0.09	0.08	0.08	0.075	1.09	0.28	0.25	0.20	0.21
Sum (mg L ⁻¹)	7.80	7.43	6.97	5.77	5.64	3.24	9.18	2.33	2.17	1.92	1.94
6-ring PAH											
INP (mg L ⁻¹)	1.12	0.98	0.96	0.81	0.82	0.76	0.17	0.08	0.06	0.05	0.05
BPR (mg L ⁻¹)	0.58	0.51	0.55	0.46	0.41	0.42	0.43	0.17	0.16	0.08	0.08
Sum (mg L ⁻¹)	1.70	1.49	1.51	1.27	1.23	1.18	0.60	0.25	0.22	0.13	0.13
∑ PAH (mg L ⁻¹)	365	340	331	289	288	209	418	111	108	82.1	80.4
Degradation (%)	–	7.3	9.6	26.9	27.9	44.7	–	73.5	75.7	82.1	81.6
Costs(\$ m ⁻³)		0.41	0.51	0.70	0.89	1.28		1.84	3.34	5.11	8.78

3.3 NAP and PYR solubilization in CAS solution

The first set of experiments consisted to determine the best way of solubilizing NAP and PYR (analytical grade reagents), respectively using an amphoteric surfactant (CAS). Different molar concentrations of CAS (0.08–27.1 g L⁻¹) were tested with a constant amount of NAP (0.1 g) and PYR (0.1 g) added in the reactor during the tests. The results are shown in Fig. 2. At low concentrations of CAS (<2.5 g L⁻¹), the NAP and PYR solubility remained very low (PAH concentration almost below detection limit). This can be attributed to the fact that, the amount of CAS was not sufficient to reach the critical point to initiate micelle formation (Critical micelle concentration, CMC), 2.5 g L⁻¹ and subsequent micelle–PAH

complex formation allowing an effective PAH solubilization. However, when the CAS concentration increased from 5.0 to 27 g L⁻¹, the micelle formation increased and the concentration of both (NAP and PYR) increased linearly. The concentration of NAP increased with a relatively high slope compared to that recorded for PYR. For the same concentration of CAS, NAP was more solubilized than PYR. It is well-known that, as the number of aromatic of PAH increases, the solubility in solution decreases. This is one the reason for which PYR (4-ring PAH) was less solubilized than NAP (2-ring PAH). It can be interesting to calculate the MSR and compared to the values with those obtained under different experimental conditions. The molar solubilisation ratio (MSR) can be defined as follows [38]:

Table 4 Influence of initial pH during the treatment of COS using either Fenton oxidation or electrochemical oxidation

PAH	Fenton oxidation ^a						Electrochemical oxidation ^b				
	Initial	pH adjustment					Initial	pH adjustment			
		2.6	4.0	5.8	7.0	9.0		2.0	4.0	7.0	9.0
2-ring PAH											
NAP (mg L ⁻¹)	25.3	7.81	6.23	8.81	8.26	12.2	72.4	14.1	13.0	10.9	16.7
MEN (mg L ⁻¹)	32.5	17.8	17.5	18.4	21.5	20.4	69.0	11.3	9.70	7.88	13.7
Sum (mg L ⁻¹)	57.8	25.6	23.7	27.2	29.7	32.6	141	25.4	22.7	18.8	30.4
3-ring PAH											
ACN (mg L ⁻¹)	2.10	0.93	0.85	1.08	0.96	1.01	3.25	0.78	0.76	0.59	0.83
ACA (mg L ⁻¹)	58.0	23.2	23.4	24.2	29.4	26.8	75.3	11.9	11.9	9.19	14.3
FLU (mg L ⁻¹)	40.0	17.8	18.1	19.9	20.6	20.8	50.1	11.7	10.5	9.48	12.0
PHE (mg L ⁻¹)	67.6	37.6	38.6	46.8	34.4	39.2	113	22.4	24.6	17.3	22.7
ANT (mg L ⁻¹)	12.3	5.09	5.23	5.73	7.19	6.32	13.3	2.36	2.25	2.06	2.91
Sum (mg L ⁻¹)	180	84.6	86.2	97.7	92.6	94.1	255	49.1	50.0	38.6	52.8
4-ring PAH											
FLU (mg L ⁻¹)	36.9	24.4	23.6	25.4	29.3	25.7	55.1	13.4	10.9	8.34	12.5
PYR (mg L ⁻¹)	36.8	17.3	17.2	17.4	23.3	18.8	35.4	9.49	7.65	6.50	8.81
BAA (mg L ⁻¹)	11.2	5.49	5.50	6.65	5.89	6.21	7.94	1.26	1.29	1.41	2.24
CHR (mg L ⁻¹)	5.90	5.21	4.80	5.81	5.49	5.65	9.70	2.35	2.09	2.34	2.92
Sum (mg L ⁻¹)	90.8	52.4	51.1	55.3	64.0	56.4	108	26.5	21.9	18.6	26.5
5-ring PAH											
BJK (mg L ⁻¹)	6.21	3.60	3.20	4.41	3.95	3.20	4.94	1.24	1.41	0.58	1.55
BAP (mg L ⁻¹)	4.82	2.73	2.41	2.82	2.51	2.92	1.56	0.26	0.26	0.19	0.27
DAN (mg L ⁻¹)	1.12	0.65	0.45	0.57	0.69	0.55	1.00	0.25	0.24	0.23	0.34
Sum (mg L ⁻¹)	12.2	6.98	6.06	7.80	7.15	6.67	7.50	1.75	1.91	1.00	2.16
6-ring PAH											
INP (mg L ⁻¹)	0.12	0.08	0.08	0.07	0.08	0.08	0.30	0.06	0.05	0.04	0.07
BPR (mg L ⁻¹)	0.61	0.39	0.39	0.44	0.43	0.38	0.30	0.08	0.05	0.06	0.06
Sum (mg L ⁻¹)	0.73	0.47	0.47	0.51	0.51	0.46	0.60	0.14	0.10	0.10	0.13
∑ PAH (mg L ⁻¹)	342	170	168	189	194	190	513	103	96.7	77.1	112
Degradation (%)	–	45.9	48.9	41.5	40.1	42.0	–	78.4	80.2	83.6	75.7

$$MSR = \frac{C_O - C_{O,CMC}}{C_S - C_{CMC}} \quad (1)$$

where “C_O” is the molar concentration of organic compound in surfactant solution, “C_S” is the surfactant concentration at which C_O is evaluated, and “C_{O,CMC}” is molar concentration of organic at C_{CMC}. The MSR can be determined from the slope of solubility curve beyond the CMC when concentration is expressed in molarities. MSR values of NAP and PYR obtained for CAS are 0.176 and 0.033, respectively, in the investigated range of 0.08–27.2 g CAS L⁻¹. The MSR value for NAP was five times higher than that recorded for PYR, confirming the relatively high solubility of NAP compared to PYR.

3.4 Effectiveness of electrooxidation in treating synthetic NAP and PYR solutions

Experiments were carried out using the electrolytic cell described in Fig. 1 at a current density of 9.23 mA cm⁻² for different treatment time (30, 60, 90 and 180 min). The rates of NAP and PYR degradation were obtained by subtracting the residual concentration from the initial value recorded in solution and the resulting operation was divided by the same initial concentration of NAP and PYR, respectively. Figure 3 shows time course changes in the normalized concentration of NAP and PYR. The initial NAP and PYR concentrations imposed during these tests were 106 mg L⁻¹ and 54 mg L⁻¹, respectively. Residual NAP and PYR concentration decreased rapidly over

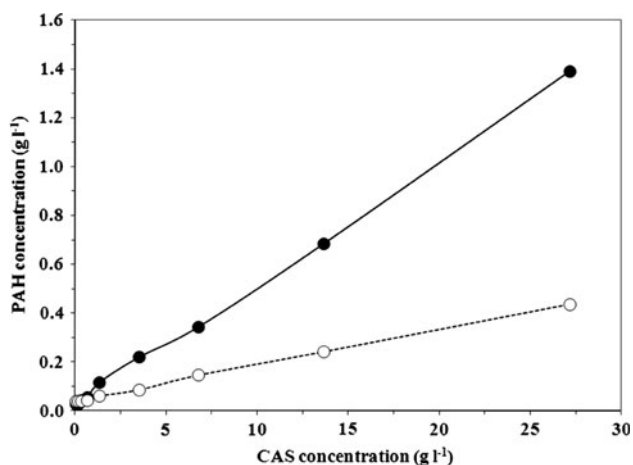


Fig. 2 Solubilization of NAP and PYR by CAS surfactant: (filled circle) NAP; (open circle) PYR

90 min of the treatment and then remained quite stable until the end of experiment (Fig. 3). NAP concentration decreased from 106 to 22 mg L⁻¹ after 90 min, which corresponded to 79% of NAP removal. By comparison, PYR concentration varied from 54 to 14 mg L⁻¹, which corresponded to 74% of PYR degradation. The rates of PYR and NAP degradation while treating individually NAP and PYR solutions were quite similar to those recorded in COS, 69–84% and 72–82%, respectively. The reaction order and the rate constant of NAP and PYR can be determined by plotting Ln (C/C₀) against time (t) (Fig. 3). The experimental data of NAP are fitted well to first-order kinetics (with correlation coefficients of 0.97) predicting a linear variation with elapsed time (t) of the -Ln (C/C₀) (Eq. 2). However, the data of PYR did not fit well to first order kinetic (with correlation coefficients of 0.78).

$$-\ln\left(\frac{C}{C_0}\right) = k.t \tag{2}$$

where “C₀” and “C” represent, respectively the initial and residual NAP or PYR concentration in the bulk solution and “k” is the first-order rate coefficient. The reaction rate constants for NAP degradation was 0.015 min⁻¹. It is interesting to compare the reaction rate constant of NAP degradation in synthetic solution with those obtained by others authors under different experimental conditions. The reaction rate constant of organic compound degradation has been determined by Kim et al. [39] while studying electrochemical oxidation of polyvinyl alcohol (PVA) using titanium coated with ruthenium oxide (Ti/RuO₂). The constant rate decreased from 0.0162 min⁻¹ to 0.0021 min⁻¹ while increasing initial PVA concentration from 33 to 2400 mg L⁻¹, using a current density of 1.34 mA cm⁻² and 0.61 g Cl⁻ L⁻¹. The smaller the initial PVA concentration,

the faster it could be removed from solution by anodic oxidation. The kinetic rate constant was the same order of magnitude in the present study and in the study carried out by Kim et al. [39] for low concentration of pollutants.

The effectiveness of the electrooxidation system was also evaluated by measuring the residual COD concentration in the solution throughout the course of the treatment. Figure 4 shows time course changes in the normalized COD concentration while treating synthetic NAP and PYR solutions. The initial COD concentration of NAP and PYR solutions during these assays were 1188 mg L⁻¹ and 1271 mg L⁻¹. For both solutions, COD decreased in the same fashion. At the end of the treatment (after 180 min), the COD reduction was 46% using either NAP or PYR synthetic solution. The results are also summarized in Table 4. The relatively low yield of COD removal (46%) compared to 94 and 80% of NAP and PYR degradation, indicated that only a small fraction of pollutants were completely oxidized into water and carbon dioxide, the majority of the pollutants being transformed into small molecules that consume oxygen in the treated-solution. In our experimental conditions, direct anodic oxidation was

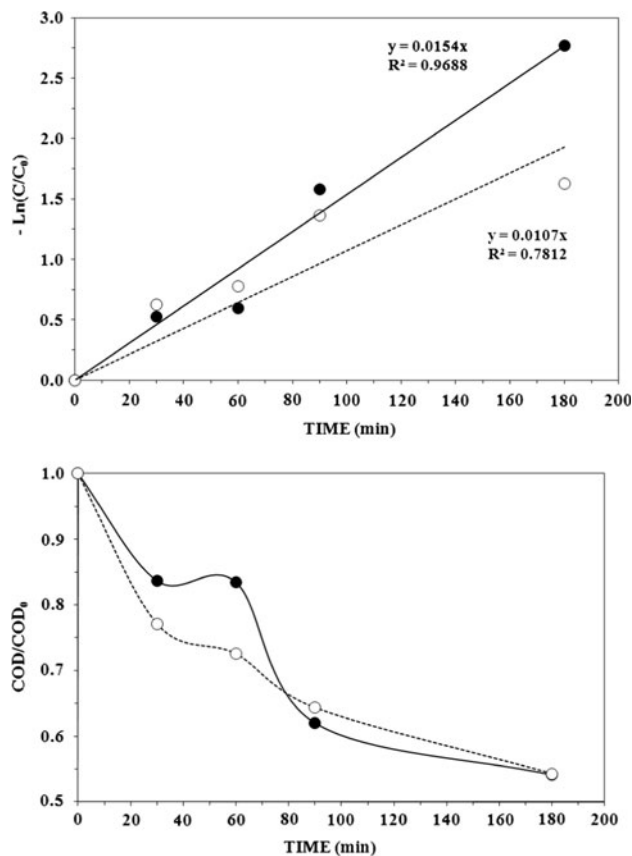


Fig. 3 Degradation kinetics of NAP and PYR in CAS solutions during electrochemical treatment operated at 9.23 mA cm⁻²; Initial NAP = 106 mg L⁻¹; Initial PYR = 54 mg L⁻¹: (filled circle) NAP; (open circle) PYR

Fig. 4 Chromatograms extracts obtained before, during (60 min) and after (90 min) by CAS electrooxidation. Current density = 9.23 mA cm^{-2} ; $[\text{Na}_2\text{SO}_4] = 0.5 \text{ mg L}^{-1}$; $[\text{CAS}] = 1 \text{ g L}^{-1}$

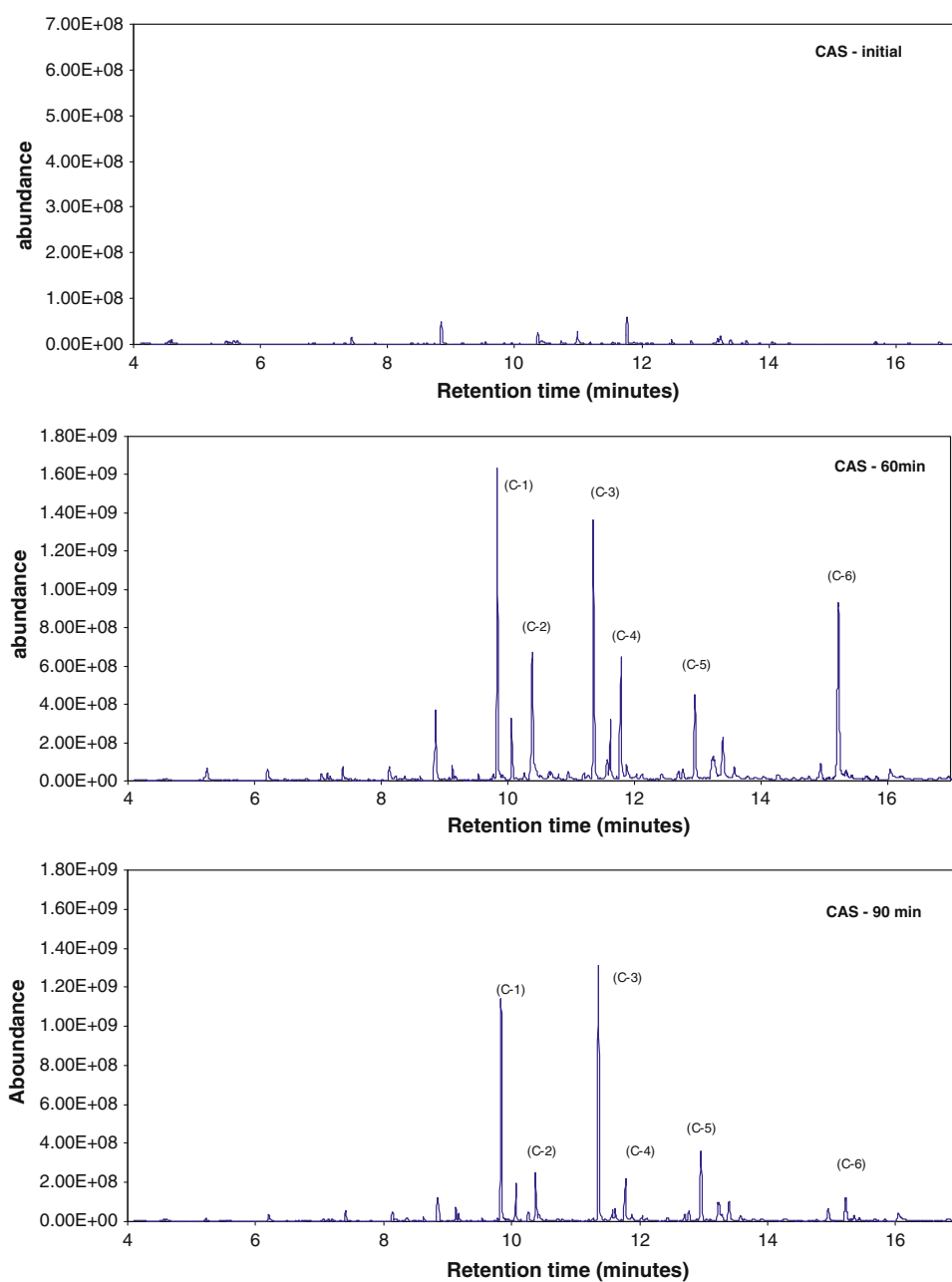


Table 5 Composition residual concentration (mg L^{-1}) depending on the reaction time

Matrixes	Parameters	Electrochemical treatment (min)					Removal (%)
		0	30	60	90	180	
NAP + CAS	NAP	106	62.5	58.4	21.8	6.64	94
	COD	1188	994	991	737	643	46
	Cl^-	57.8	54.3	51.5	48.5	41.0	29
PYR + CAS	PYR	54.1	29.0	24.8	13.8	10.6	80
	COD	1271	980	922	818	690	46
	Cl^-	56.1	50.6	47.9	45.4	37.0	34
CAS	COD	1095	916	904	859	821	25
	Cl^-	55.9	50.0	49.5	47.2	40.8	27

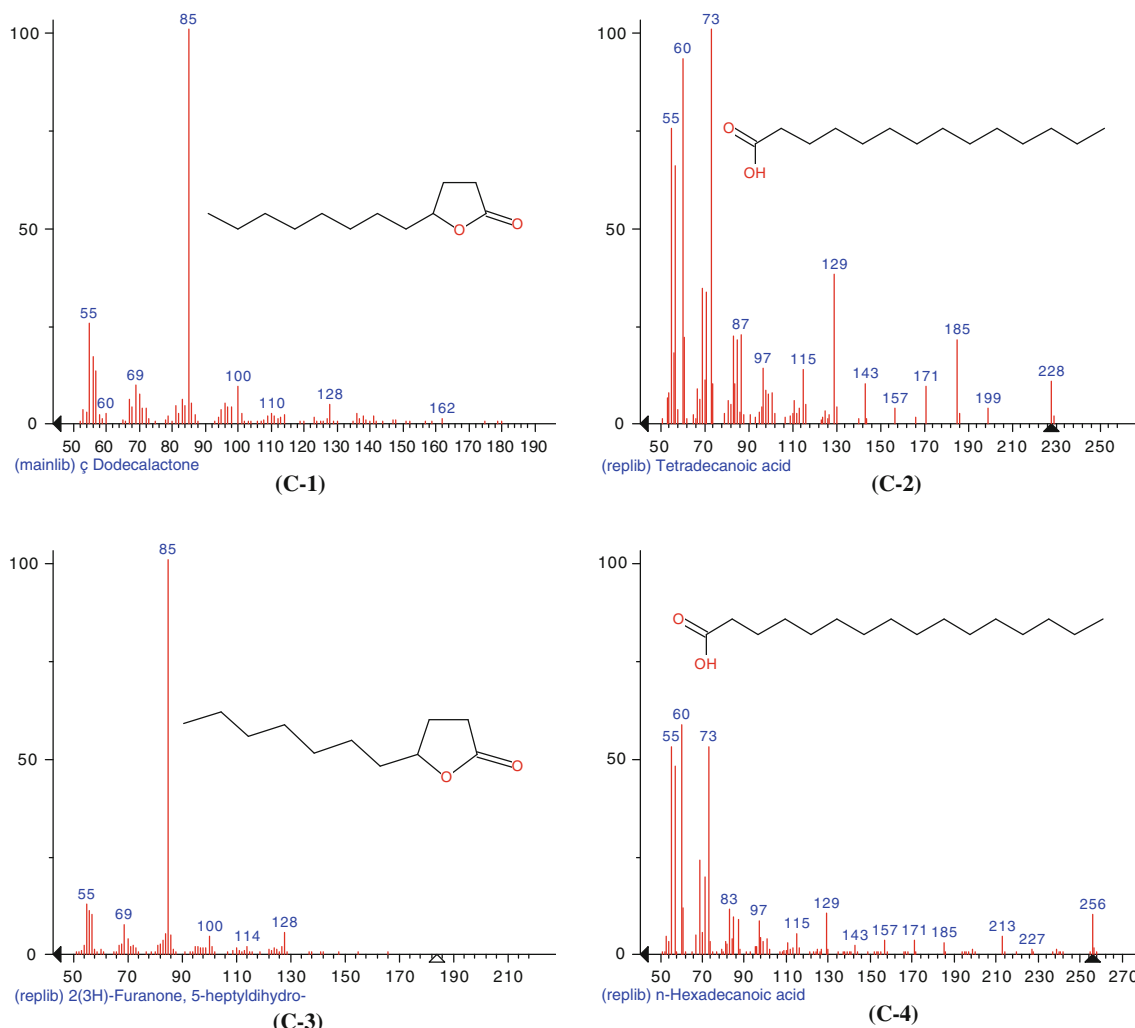


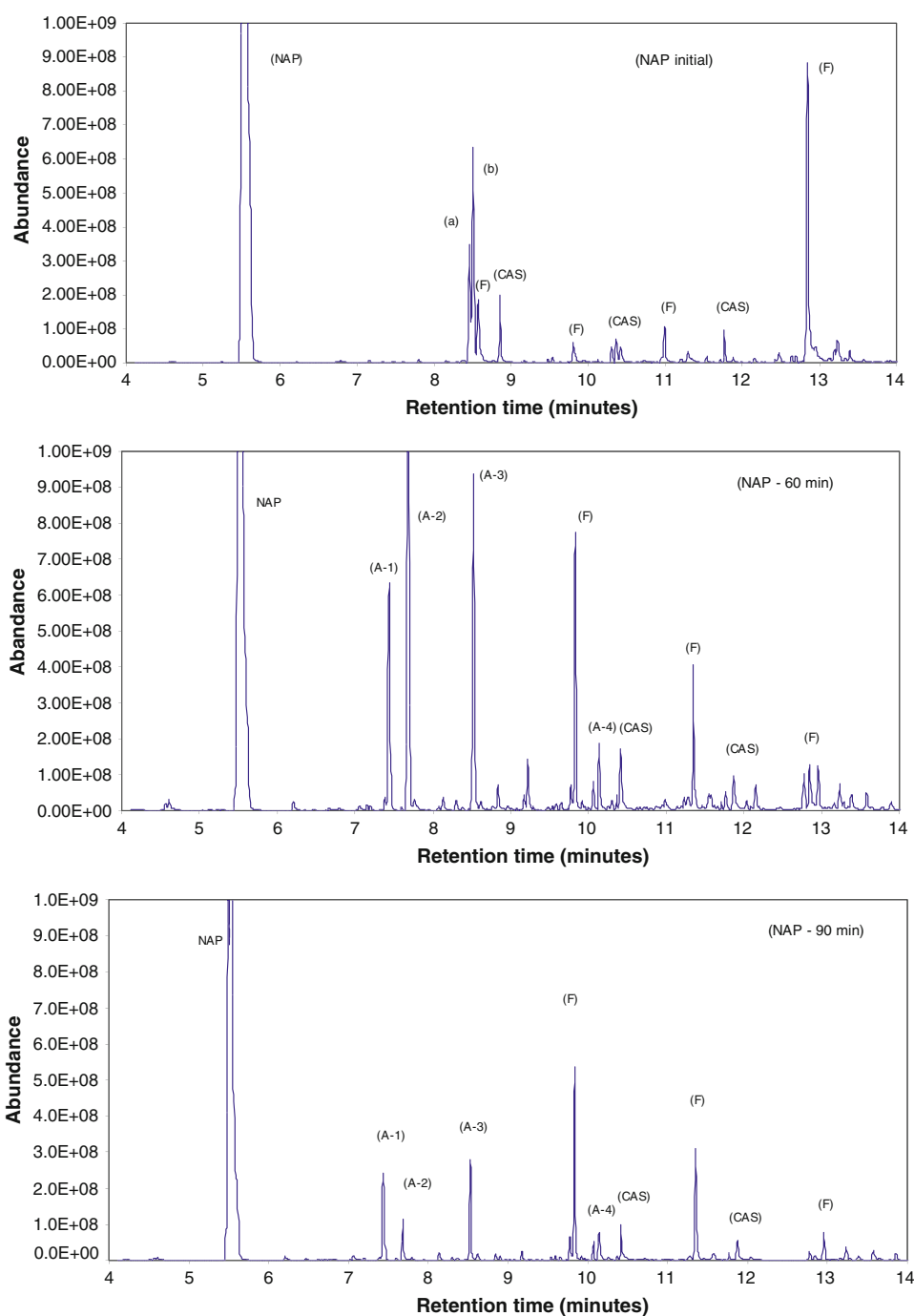
Fig. 5 Mass spectra of some by-products of CAS electrooxidation

the predominant reaction. However, indirect oxidation may have taken place owing to the presence of chloride ions measured in the synthetic solutions. As it can be seen from Table 5, chloride ions were originated from CAS solution. Chloride concentration varied from the initial value around 56–58 mg L⁻¹ to the final values varying from 37 to 41 mg L⁻¹ (27–34% of chloride consumption) owing probably to chloride ions oxidation at the anode (Ti/RuO₂) electrodes to chlorine gas. The chlorine gas reacts immediately with water to form hypochlorous acid (HClO) [40, 41].

In general, the oxidation of chloride ion can be observed on DSA, such as Ti/RuO₂ [40]. In dilute chloride solution, a parallel reaction occurs on such anode electrode concomitant with the formation of chlorine, i.e., hydroxyl radical and oxygen evolution reactions. Likewise, from Table 5, it can also be seen that, 25% of COD was removed while only CAS solution was submitted to electrolysis. It is

also possible from Table 5 to make approximate calculations and see whether or not the non-degradable COD was from CAS while electrolyzing individual NAP and PYR solutions. For instance, an initial COD concentration of 1271 mg L⁻¹ was recorded while the mixture comprised of PYR and CAS was prepared. By comparison, when CAS solution was prepared alone, an initial COD concentration of 1095 mg L⁻¹ was measured. Thus, in the PYR + CAS matrix, 14% of COD was due to PYR compound, whereas 86% was attributed to CAS alone. The percentage of PYR contribution to the COD measurement was estimated by subtracting the COD concentration of the PYR + CAS matrix from the COD concentration of the CAS solution divided by the total COD of the mixture comprised of PYR and CAS. At the end of electro-oxidation treatment of PYR + CAS matrix, a residual COD concentration of 690 mg L⁻¹ was recorded, 14% of this value being attributed to PYR alone (97 mg L⁻¹) versus 86% for CAS

Fig. 6 Chromatograms extracts obtained before, during (60 min) and after (90 min) of NAP electrooxidation in CAS surfactant solution. Current density = 9.23 mA cm^{-2} ; $[\text{Na}_2\text{SO}_4] = 0.5 \text{ mg L}^{-1}$; $[\text{CAS}] = 1 \text{ g L}^{-1}$



alone (593 mg L^{-1}). Consequently, most of the non-degradable COD was from CAS. For NAP + CAS matrix, the same trend can be observed.

Degradation of surfactant (anionic and cationic surfactant) using electrochemical technology has been also carried out by Lissens et al. [41] and Panizza et al. [42]. Direct anodic oxidation of sodium dodecyl benzene sulfonate and hexadecyltrimethyl ammonium chloride has been studied using BDD electrode in batch electrolysis mode operated at a current density of 4 mA cm^{-2} . 83% TOC removal has

been recorded for sodium dodecyl benzene sulfonate by Lissens et al. [41], whereas 68% of TOC removal has been measured for the hexadecyltrimethyl ammonium chloride surfactant.

3.5 By-products formation

Our intention is to follow the formation of some by-products, and possibly identify some chemical structures while treating synthetic solutions containing NAP and PYR,

Table 6 By-products of NAP electrooxidation identified by GC–MS

Products	RT ^a	MW ^b	Peaks	Abundance (min)		
				0	60	90
Naphthalene	5.54	128		52×10^8	38×10^8	23×10^8
Chloronaphthalene	7.43	162	(A-1)		6.3×10^8	2.4×10^8
1,4-naphthalenedione	7.68	158	(A-2)		14×10^8	1.2×10^8
2-naphthol	8.46	144	(a)	3.5×10^8	$<10^7$	$<10^7$
1-naphthol	8.50	144	(b)	6.4×10^8	$<10^7$	$<10^7$
1,4-naphthoquinone 2,3-oxide	8.52	174	(A-3)		9.4×10^8	2.7×10^8
Undecanoic acid	8.86	186	(CAS)	2.0×10^8	$<10^7$	$<10^7$
Furanone	9.83	85	(F)	0.5×10^8	7.7×10^8	5.4×10^8
2-Ethoxyquinoline	10.15	173	(A-4)		1.9×10^8	0.8×10^8
Decanamide	10.42	143	(CAS)		1.7×10^8	1.0×10^8
Octanamide, <i>N,N</i> -dimethyl	10.98	171	(CAS)	1.0×10^8	$<10^7$	$<10^7$
Furanone	11.35	85	(F)		4.0×10^8	3.1×10^8
Tetradecanamide	11.87	198	(CAS)	1.1×10^8	1.0×10^8	0.5×10^8
Furanone	12.96	85	(F)	8.8×10^8	1.2×10^8	0.8×10^8

^a Retention time (min)^b Molecular weight

respectively. The first tests were carried out in order to verify if the CAS was oxidized during electrolysis. The electrolysis cell was operated at a current density of 9.23 mA cm^{-2} though 90 min of treatment in the presence of $0.5 \text{ g Na}_2\text{SO}_4 \text{ L}^{-1}$ with initial pH adjustment around 6.4 (to have the same initial conditions while electrolysing NAP and PYR synthetic solution). The GC–MS results of the intermediate products for CAS are presented in Figs. 4 and 5. After 60 min of electrolysis, four important peaks (C-1, C-2, C-3 and C-4) appeared in the gas chromatogram and represented the intermediate products. They were analyzed in detail by mass spectroscopy (Fig. 5). These components C-1, C-2, C-3 and C-4, respectively corresponded to n-hexadecanoic acid, decanenitrile, 1-dodecanethiol, and furanone, 5-dodecyldihydro (by comparison of mass spectra with those of NIST mass spectra library). It could be seen that the concentration of these four intermediates increased during the first 60 min of the electrooxidation process, and then decreased with electrooxidation time, after 90 min of treatment. They all drop to a very low concentration. It can be concluded that all these four intermediates were generated during the initial steps and when the electrooxidation process pursued, they were gradually oxidized. Likewise, some compounds such as furanone (having low molecular weight) appeared during electrolysis.

Subsequently, a synthetic solution containing NAP was electrolysed and the formation of some by-products was identified. A typical GC pattern of dichloromethane extract, containing residual NAP and various reaction intermediates present in the electrolysed solution after 60

and 90 min is shown in Fig. 6, where compound related to the starting pollutant show retention time in the range 5–14 min. Among the peaks observed, some corresponded to single products, whereas others were subjected to interference and required MS identification and monitoring. The identified results for NAP electro-degradation depend on reaction time (0, 60 and 90 min). The analysis of the initial NAP (before electrolysis) shows several peaks ((a) (b) (F) (CAS) and (NAP) peaks) identified and characterized in Table 6. By comparison, the peaks (A-1) (A-2) (A-3), and (A-4) in the gas chromatogram were the intermediate products and were analyzed in detail by mass spectroscopy (see Fig. 7) after 60 and 90 min of period of electrolysis. These components (A-1) (A-2) (A-3), and (A-4), respectively corresponded to chloronaphthalene, 1,4 naphthalenedione, 1,4-naphthoquinone and 2-ethoxyquinoline (by comparison of mass spectra with those of NIST mass spectra library). A list of identified compounds together with their observed relative abundance in the extract is given in Table 6. From the gas chromatogram, it could be seen that these four intermediates increased to a relatively high concentration during the first 60 min of the electrooxidation process, and then decreased with electrooxidation time, after 90 min of treatment. They all drop to a very low concentration. It can be concluded that all these four intermediates were generated during the initial steps and when the electrooxidation process pursued, they were gradually oxidized. From Table 6, it can be seen that naphthoquinone was one of the main by-products generated during electrooxidation process. Similar results have been recorded while studying oxidative degradation processes of

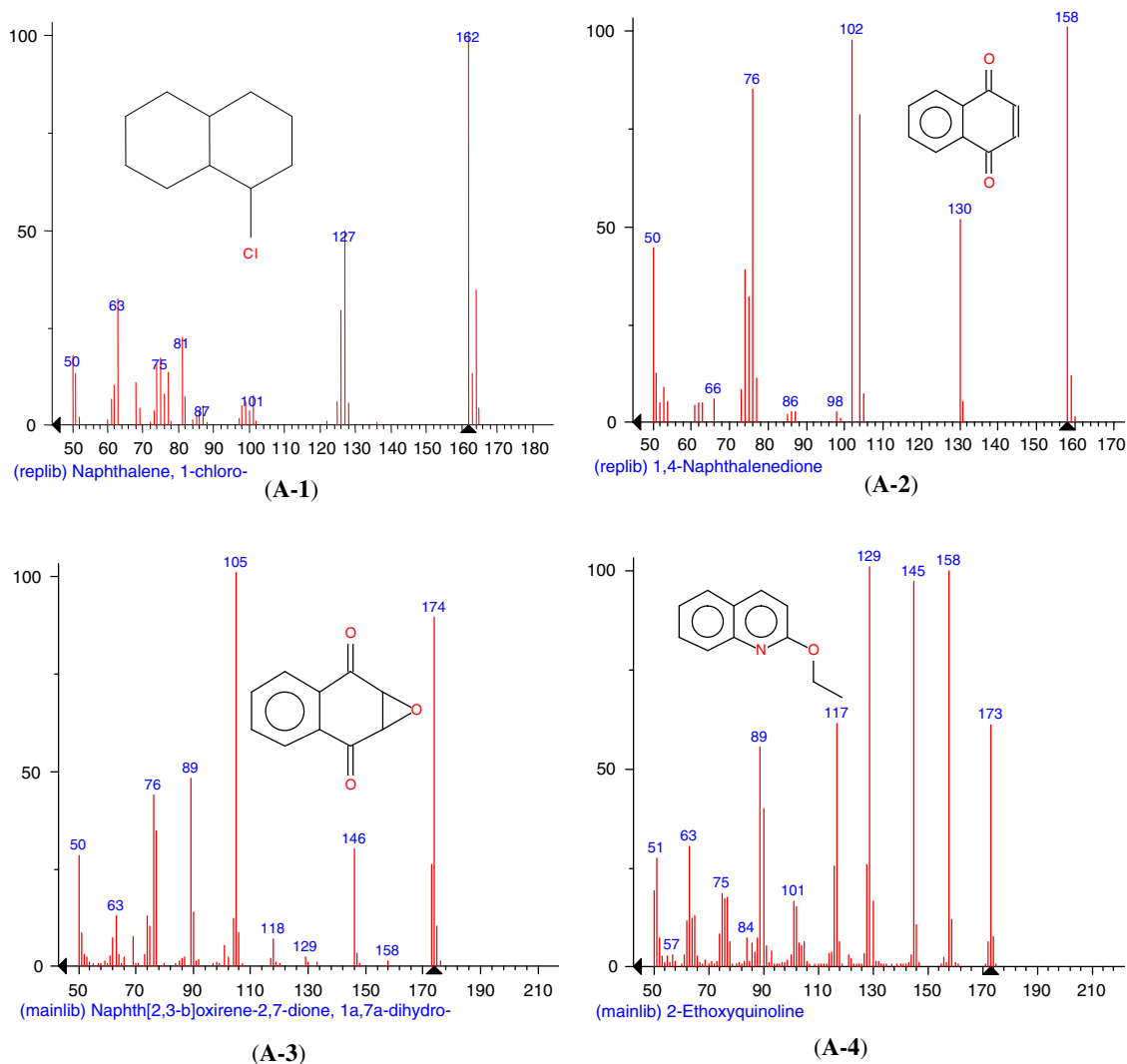


Fig. 7 Mass spectra of components (A-1) (A-2) (A-3) and (A-4) produced by NAP electrooxidation

NAP using both photoinduced in Fe(III) solution and photocatalyzed by Q-TiO₂ colloids [43]. The primary degradation intermediates (2-formylcinnamaldehyde, 1,2-naphthoquinone, 1,4-naphthoquinone, 1-naphthol, 2-naphthol) were the same regardless of the photocatalysis system used. Another study showed that naphthoquinone was formed as intermediate product while treating NAP synthetic solution using indirect electrooxidation process where a mediator (Ce^{III}/Ce^{IV}) is electrochemically generated to carry out the oxidation of the pollutant [44].

The GC-MS results of the intermediate products for PYR are presented in Fig. 8 and Table 7. The peaks (B-1) (B-2), and (B-3) in the gas chromatogram were the intermediate products and were analyzed by mass spectroscopy (Fig. 9). These components (B-1) (B-2), and (B-3), respectively corresponded to chloropyrene, benzo[*c*]cinnoline-2 chloro and sulfonyl-bis (2-nitroxidophenyl),

which were determined in conformity with NIST mass spectra library. The intermediates increased to a relatively high concentration at the start of the electrooxidation experiment, and then decreased with time, after 90 min of period of treatment. In particular, chloropyrene (B-2) drop to a very low concentration. It can be concluded that chloropyrene was generated during the initial steps and when the electrooxidation process pursued, it was gradually oxidized. PYR degradation was also studied by Wen et al. [45] by using photocatalytic oxidation technique where PYR was preadsorbed on TiO₂. According to these authors, the ring-open reaction, hydroxylation and ketolysis occurred to produce some intermediate products (such as 4-oxapyrene-5-one, 1,6 or 1,8 pyrenediones, 4,5-phenanthrenedialdehyde and cyclopenta[*def*]phenanthrene). These intermediates were different to those recorded in the present study while treating PYR synthetic solution.

Fig. 8 Chromatograms extracts obtained before, during (60 min) and after (90 min) of PYR electrooxidation in CAS surfactant solution. Current density = 9.23 mA cm^{-2} ; $[\text{Na}_2\text{SO}_4] = 0.5 \text{ mg L}^{-1}$; $[\text{CAS}] = 1 \text{ g L}^{-1}$

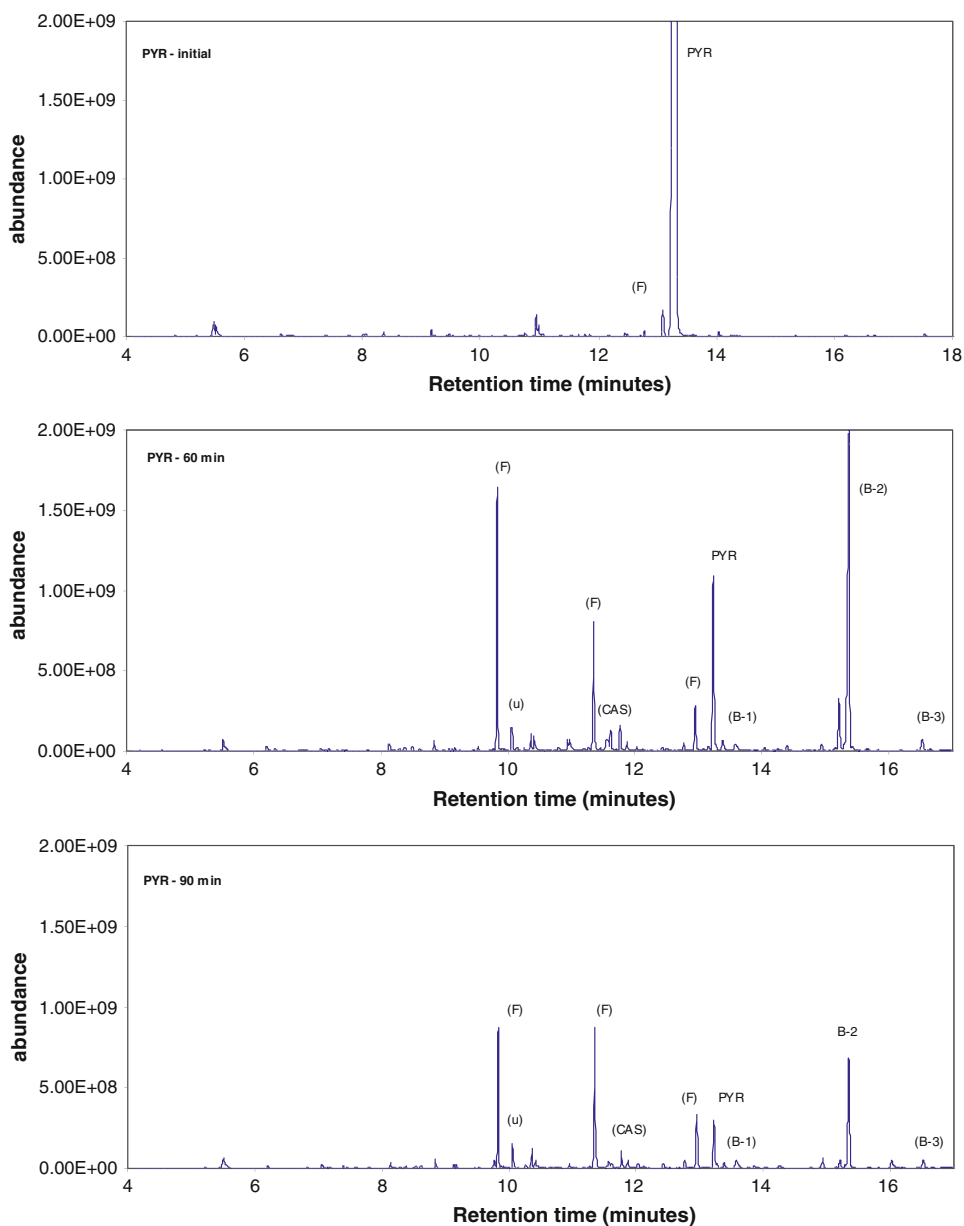


Table 7 By-products of PYR electrooxidation identified by GC-MS

Products	RT	MW	Peaks	Abundance (min)		
				0	60	90
Furanone	9.83	85	(F)		16×10^8	8.7×10^8
Unknown	10.06	99	(u)		1.5×10^8	1.5×10^8
Furanone	11.34	85	(F)		8.0×10^8	8.6×10^8
Hexadecanoic acid	11.77		(CAS)		1.6×10^8	1.1×10^8
Furanone	12.95		(F)		2.9×10^8	3.1×10^8
Pyrene	13.23		PYR	11.6×10^9	10.8×10^8	2.3×10^8
Benzo(c)cinnoline, 2-chloro	13.58		(B1)		0.2×10^8	0.2×10^8
Chloropyrene	15.34		(B2)		19.8×10^8	6.7×10^8
Sulfonyl-bis (2-nitroxidophenyl)	16.53		(B3)		0.7×10^8	0.3×10^8

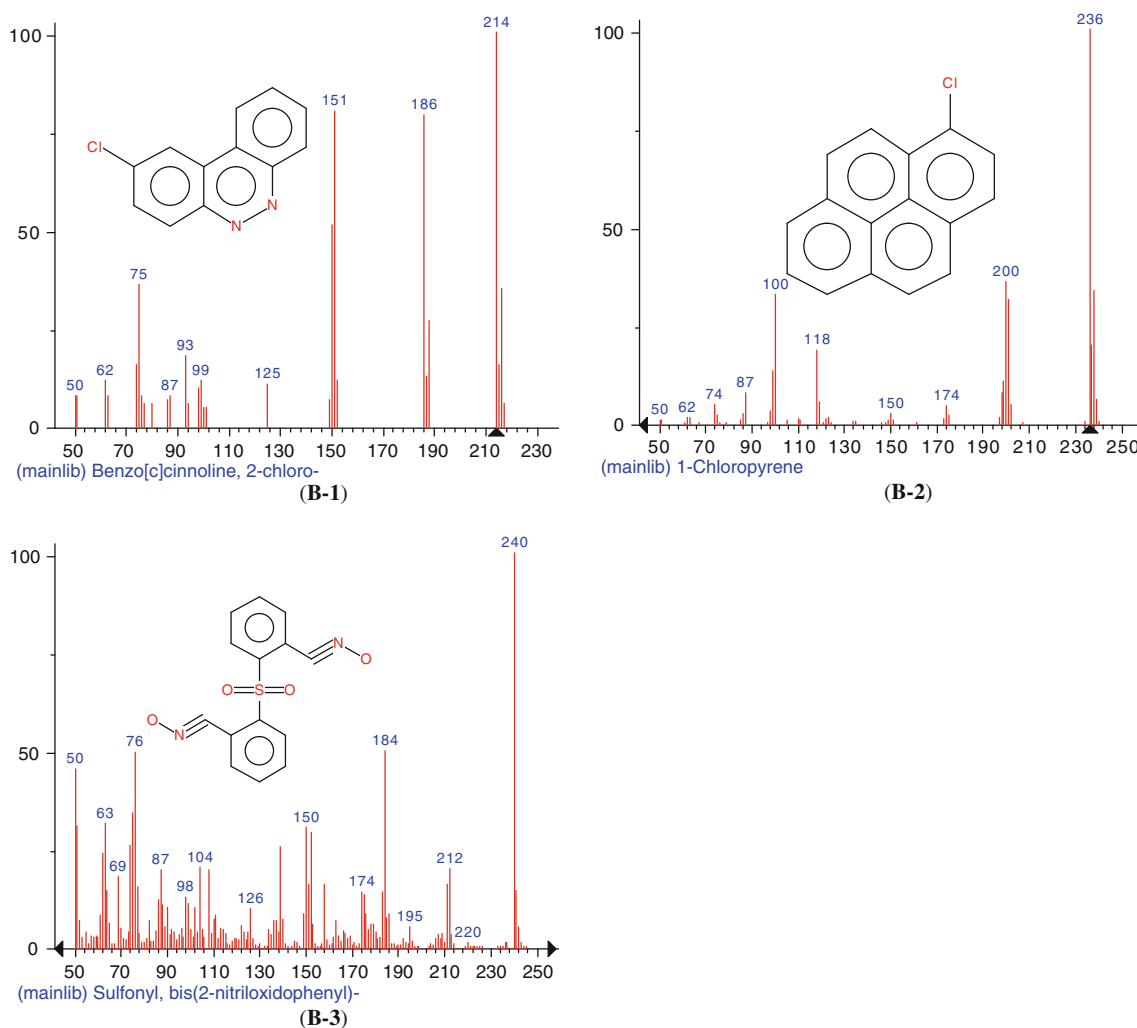


Fig. 9 Mass spectra of components **(B-1)** **(B-2)** and **(B-3)** produced by PYR electrooxidation

3.6 Proposed mechanisms of NAP and PYR degradation

Based on the found primary intermediates, reaction pathways of the NAP degradation can be proposed (Fig. 10). Firstly, hydroxyl radical produced on anode electrode reacts with NAP and leads to the formation of 1,4-naphthalenedione (A-2). Subsequently, 1,4-naphthalenedione is oxidized by hydroxyl radical and 1,4-naphthoquinone (A-3) is formed. Naphthoquinone compounds should consecutively transform via next attacks of hydroxyl radical into further intermediates, including ring-opened structures. The subsequent oxidation of the ring-opened structure may result in fully oxidized reaction products and leads to the formation of carbon dioxide (CO₂). This hypothesized CO₂ formation is based on the results described elsewhere [46]. In the previous study, the performance of the electrolytic cell has been evaluated by the measurements of both DOC and TOC while treating

synthetic solution containing various concentration of PAH. The yields of DOC and TOC removal were 62% and 27%, respectively. The relatively low yield of TOC removal (27%) compared to 62% of COD removal, indicated that only a small fraction of PAH was completely oxidized into water and carbon dioxide, the majority of the pollutants being transformed into small molecules that reduce the oxygen demand in the treated-solution relative to the achieve removal of the original compounds. Another pathway of NAP degradation proposed in the Fig. 10 is based on the possibility of the formation of hypochlorous acid (generated via chloride ion oxidation at the anode) during electrolysis, which can then react with NAP to form chloronaphthalene (A-1), followed by rearomatization and formation of 2-ethoxyquinoline (A-4). Ethoxyquinoline should be subsequently transformed via next attacks of hydroxyl radical into further intermediates, including ring-opened structures. On the other hand, NAP could be directly oxidized into ethoxyquinoline (A-4). According to

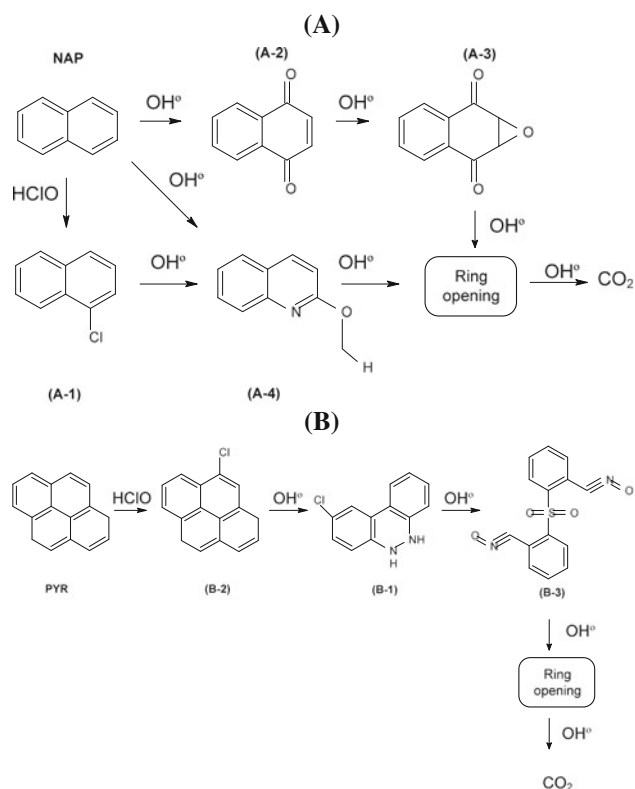


Fig. 10 NAP (a) and PYR (b) electrooxidation pathways in the presence of CAS

the primary intermediates found during electrolysis of PYR solution, reaction pathways of the PYR degradation can also be proposed. Chloropyrene (B-2) is generated owing to hypochlorous acid reaction with PYR, followed by rearomatization and formation of benzo(c)cinnoline, 2-chloro (B-1). Benzo(c)cinnoline, 2-chloro can then be oxidized by hydroxyl radical to form sulfonyl-bis (2-nitriloxidophenyl) (B-3), which should be consecutively transformed into further intermediates, including ring-opened structures.

4 Conclusions

This study has shown the possibility to use an electrochemical technique to oxidize efficiently PAH from COS and from NAP and PYR synthetic solutions in comparison to traditional Fenton oxidation process. Using electrochemical oxidation, the sum of PAH concentrations for 16 PAHs investigated in COS could be optimally diminished up to 80–82% by imposing a current density of 9.23 mA cm^{-2} and a pH of 4.0 or 7.0 for 90-min reaction period in the electrolysis cell. By comparison, the best yield (46%) of Fenton oxidation process for PAH

degradation in COS was recorded while imposing $\text{H}_2\text{O}_2/\text{Fe}^{2+}$ molar ratio of 11.0 (with $1.7 \text{ mol Fe}^{2+} \text{ L}^{-1}$) and a pH of 4.0. Individual NAP and PYR solutions were then oxidized electrochemically in order to monitor the formed intermediates. The rates of PYR and NAP degradation while treating individually NAP and PYR solutions were quite similar to those recorded in COS (79% of NAP removal and 74% of PYR removal). NAP is mainly transformed via direct oxidation. Naphthalenedione and naphthoquinone are successively formed through the oxidation induced by hydroxyl radicals and naphthoquinone should consecutively transform into further intermediates, including ring-opened structures. During oxidation of PYR solution, PYR is mainly transformed to chloropyrene followed by rearomatization and formation of benzo(c)cinnoline, 2-chloro. Benzo(c)cinnoline, 2-chloro is then be oxidized by hydroxyl radical to form sulfonyl-bis (2-nitriloxidophenyl). The electro-oxidation technique could form the basis of a process capable of removing refractory organic compounds such as PAHs from many wastes and wastewaters (creosote effluent, petroleum effluent, aluminum industry wastes and soil wastes, etc.). However, in view of verifying the effect of treatment time on Fenton oxidation process and with the aim of confirming the most cost-effective process for treating COS (electro-oxidation versus Fenton oxidation), additional experiments using response surface methodology (RSM) should be used.

Acknowledgments Sincere thanks are extended to the Canada Research Chairs and to the National Sciences, Engineering Research Council of Canada and Filter Innovations Inc. for their financial to this study.

References

1. Sigman ME, Schuler PF, Ghosh MM, Dabestani RT (1998) *Environ Sci Technol* 32:3980
2. Flotron V, Delteil C, Pedellec Y, Camel V (2005) *Chemosphere* 59:1427
3. USEPA (1984) Creosote—special review position. Document 2/3. U.S. Environmental Protection Agency, Washington, DC
4. Betts WD (1990) Information about coal-tar creosote for wood. Proceedings of the international tar conference, Paris, France
5. Gouvernement of Canada (1993) *Matières résiduelles imprégnées de créosote. Loi Canadienne sur la protection de l'environnement, liste des substances d'intérêt prioritaire*. Report No. En 40-215/13-F, Ottawa, Ontario, Canada (in French)
6. Engwall MA, Pignatello JJ, Grasso D (1999) *Water Res* 33:1151
7. Becker L, Matuschek G, Lenoir D, Ketrup A (2001) *Chemosphere* 42:301
8. Ikarashi Y, Kaniwa M, Tsuchiya T (2006) *Chemosphere* 60:1279
9. Trapido M, Veressinina Y, Munter R (1995) *Environ Technol* 16:729
10. Beltrán F, González M, Rivas FJ, Alvarez P (1998) *Water Air Soil Pollut* 105:685
11. Goel RK, Flora JRV, Ferry J (2003) *Water Res* 37:891

12. Stichnothe H, Keller A, Thiming J, Lohmann N, Calmano W (2002) *Acta Hydrochimica Hydrobiologica* 30:87
13. Panizza M, Zolezzi M, Nicoletta C (2006) *J Chem Technol Biotechnol* 81:225
14. Romero MC, Cazau MC, Giorgieri S, Arambarri AM (1998) *Environ Pollut* 101:355
15. Juhasz AL, Naidu R (2000) *Int Biodeterior Biodegrad* 45:57
16. Lin SH, Lo CC (1997) *Water Res* 31:2050
17. Kang YW, Hwang KY (2000) *Water Res* 34:2786
18. Kuo WG (1992) *Water Res* 26:8801
19. Tang WZ, Huang CP (1996) *Environ Technol* 17:1371
20. Wang A, Qu J, Liu H, Ge J (2004) *Chemosphere* 55:1189
21. Martinez-Huitle CA, Ferro S (2006) *Chem Soc Rev* 35:1324
22. Deng Y, Englehardt JD (2007) *Waste Manag* 27:380
23. Morao A, Lopes A, De Amorim MTP, Goncalves IC (2004) *Electrochim Acta* 49:1587
24. Rao NN, Somasekhar KM, Kaul SN, Szyrkowicz L (2001) *J Chem Technol Biotechnol* 76:1124
25. Panizza M, Cerisola G (2004) *Environ Sci Technol* 38:5470
26. Drogui P, Blais JF, Mercier G (2007) *Recent Patent Eng* 1:257
27. Comninellis C, Pulgarin C (1991) *J Appl Electrochem* 21:703
28. Comninellis C (1994) *Electrochim Acta* 39:1857
29. Panizza M, Cristina C, Cerisola G (2000) *Water Res* 34:2601
30. Rajeshwar K, Ibanez J (1997) *Environmental electrochemistry—fundamentals and applications in pollution abatement*. Academic Press, San Diego, CA
31. Drogui P, Elmaleh S, Rumeau M, Bernard C, Rambaud A (2001) *J Appl Electrochem* 31:877
32. Bongo G, Mercier G, Drogui P, Blais JF (2008) *Environ Technol* 29:479
33. Chartier M, Dhenain A, Mercier G, Blais JF, Drogui P, Bongo G (2008) Canada Patent pending, No 2,631,092
34. Mercier G, Blais JF, Chartier M (2007) *J Environ Eng Sci* 6:53
35. Mouton J, Mercier G, Blais JF (2009) *Water Air Soil Pollut* 197:381
36. Yavuz Y, Caporal AS (2006) *J Hazard Mater B* 136:296
37. Chen X, Chen G (2006) *Sep Purif Technol* 48:45
38. Edwards DA, Luthy RG, Liu Z (1991) *Environ Sci Technol* 25:127
39. Kim S, Kim T, Park C (2003) *Desalination* 155:49
40. Matskevich ES, Slipchenko AV (1993) *Zh Prikl Khim* 66:1493
41. Lissens G, Pieters J, Verhaege M, Pinoy L, Verstraete W (2003) *Electrochim Acta* 48:1655
42. Panizza M, Delucchi M, Cerisola G (2005) *J Appl Electrochem* 35:357
43. Hykrodova L, Jirkovsky J, Mailhot G, Bolte M (2000) *J Photochem Photobiol A Chem* 151:181
44. Lund H, Hammerich O (2001) *Organic electrochemistry*. Marcel Dekker Inc., New York, NY, p 1185
45. Wen S, Zhao J, Sheng G, Fu J, Peng P (2003) *Chemosphere* 50:111
46. Tran LH, Drogui P, Mercier G, Blais JF (2009) *J Hazard Mater* 164:1118
47. Latimer JS, Zheng J (2003) In: Douben PET (ed) *PAH: an ecotoxicological perspective*. Wiley, London, England
48. Yeung KKC, Lucy CA (1997) *Anal Chem* 69:3435
49. Lucy CA, Tsang JSW (2000) *Talanta* 50:1283